ISSN 1070-3284, Russian Journal of Coordination Chemistry, 2018, Vol. 44, No. 9, pp. 565–571. © Pleiades Publishing, Ltd., 2018.

Syntheses, Crystal Structures, and Fluorescence Properties of 3*d*–4*f* Coordination Polymers LnNi (Ln = Er, Eu)[1]

G. Z. Deng[a], N. Xin[a], Y. Q. Sun[a, *], Y. Y. Xu[a], and D. Z. Gao[a]

[a] *Tianjin Key Laboratory of Structure and Performance for Functional Molecule, College of Chemistry, Tianjin Normal University, Tianjin, 300387 P.R. China*

**e-mail: hxxysyq@mail.tjnu.edu.cn*

Received January 10, 2018

Abstract—Two novel 3*d*–4*f* coordination polymers $[Ln(NiL)(Nipt)(C_2O_4)_{0.5} \cdot H_2O] \cdot H_2O$ (Ln = Er (**I**), Eu (**II**) (H_2L = 2,3-dioxo-5,6,14,15-dibenzo-1,4,8,12-tetraazacyclopentadeca-7,13-dien; H_2Nip = 5-nitroisophthalic acid) were obtained by using 5-nitroisophthalate and mononuclear macrocyclic oxamide complex NiL as co-ligand to react with $Ln(NO_3)_3 \cdot 6H_2O$ (Ln = Er, Eu) under solvothermal condition, and characterized by single crystal X-ray diffraction (CIF files CCDC nos. 1587618 (**I**) and 1587619 (**II**)). Two complexes are isostructural structure and exhibit a two-dimensional network architecture formed by [Ln(III)Ni(II)] units via the oxamide, 5-nitroisophthalate and oxalate bridges, and adjacent 2D structures are linked together with C–H···O and O–H···O intermolecular hydrogen bonds to form a 3D superamolecular architectures. The fluorescence properties of **I** and **II** are also characterized.

Keywords: 3*d*–4*f* coordination polymers, macrocyclic oxamide complex, fluorescence properties

DOI: 10.1134/S1070328418090014

INSTRODUCTION

In recent years, the 3*d*–4*f* heterometallic coordination polymers (CPs) have been attracted much attention and quickly became a hot topic because of their fascinating structures and the potential application in magnetism, luminescence, adsorption, catalysis, etc. [1–12]. Up to date, many these kinds of CPs have been synthesized by using the ligands containing both N- and O-donors to react with lanthanide and transition metal ions directly, according to the hard-soft acid based model [13–16], however, it's still difficult to control the reaction because of the competition between the lanthanide and transition metal ions in the process of self-assembly. Recently, by using benzotriazole-5-carboxylate/5-nitroisophthalate and mononuclear macrocyclic oxamide complex ML co-ligands, we have successfully obtained some 3*d*–4*f* heterometallic CPs [17], however, rational control in the construction of oxamido and multicarboxylate bridged 3*d*–4*f* polymeric networks still remain a great challenge in crystal engineering. In this paper, we also adopted the 'metalloligand' and co-ligand synthetic approach to design and synthesize novel 3*d*–4*f* CPs. Firstly, synthesize the mononuclear macrocyclic oxamide Ni(II) complex (NiL) with exo oxygen donors (Scheme 1a) [18]; then we used macrocyclic oxamide NiL units and 5-nitroisophthalate as co-ligand to react with $Ln(NO_3)_3 \cdot 6H_2O$ based on the following reasons: firstly, NiL and 5-nitroisophthalate both have oxygen donors which prefer to bond to Ln^{3+} ions simultaneously; secondly, 5-nitroisophthalate have the ability to construct CPs because of its versatile coordination modes; lastly, the nitro and carboxyl groups can potentially be used as hydrogen bond acceptors and donors to assemble supramolecular structures [17, 19, 20]. On the other hand, many complexes containing rare earth ions have good fluorescence properties [21–25], but those containing 3*d*–4*f* metals, especially 3*d*–4*f* CPs, have been investigated rarely [25, 26]. Considering the synergistic effect between lanthanide and transition metal ions and the different ligands, we investigate the fluorescence of 3*d*–4*f* CPs, which will give the basic and useful information for the development of new fluorescent materials.

With these facts in mind and in continuation of our work on 3*d*–4*f* CPs, two novel 3*d*–4*f* CPs $[Ln(NiL)(Nipt)(C_2O_4)_{0.5} \cdot H_2O] \cdot H_2O$ (Ln = Er (**I**), Eu (**II**) have been isolated and structurally characterized, the fluorescent properties of **I** and **II** are also preliminarily investigated.

The macrocyclic oxamide complex ligand (NiL) (a) and the coordinated mode of 5-nitroisophthalate (Ln = Er, Eu) (b) are shown in Scheme:

[1] The article is published in the original.

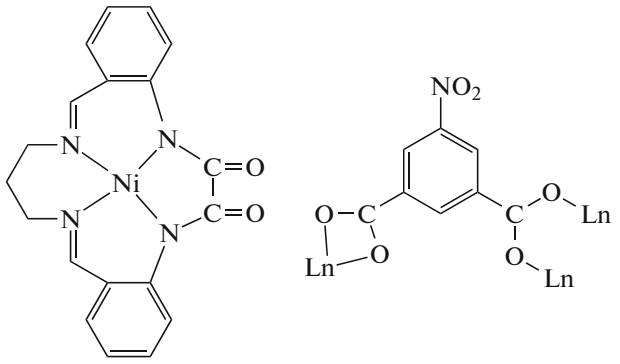

(a) **Scheme 1.** (b)

EXPERIMENTAL

Reagents were of A.R. grade and were used as purchased. The complex ligand NiL was prepared according to the reference literature [18]. Analyses of C, H and N were determined on a Perkin-Elmer 240 Elemental analyzer. IR spectrum was recorded as KBr discs on a Shimadzu IR-408 infrared spectrophotometer in the 4000–600 cm^{-1} range. Test the fluorescence properties with the RF-5301PC fluorescence.

Synthesis of $[Ln(NiL)(Nip)(C_2O_4)_{0.5} \cdot H_2O] \cdot H_2O$ (Ln = Er (I), Eu (II). At room temperature, $Ln(NO_3)_3 \cdot 6H_2O$ (0.05 mmol, Ln = Er 23.1 mg; Eu 22.3 mg), NiL (0.1 mmol, 19.6 mg), Nip (0.1 mmol, 21 mg), H_2O (10 mL) and CH_3OH (4 mL) were mixed and stirred slightly for a while. The pH value of the solution was adjusted to about 7–8 by using triethylamine aqueous solution. After stirring, transferred the mixture to a 20 mL Teflon-lined reactor, then heated from room temperature to 150°C with in 24 h, heated at 150°C for 72 h and then cooled to room temperature for 72 h. Finally, the red brown block-shaped crystals of **I** and **II** were obtained and washed several times by water.

For $C_{28}H_{23}N_5O_{12}NiEr$ (**I**)

Anal. calcd., %	C, 39.65	H, 2.76	N, 8.26
Found, %	C, 39.60	H, 2.72	N, 8.29

IR (ν, cm^{-1}): 1635 ν(COO^-), 1611 ν(C=O), 1541 ν(C=N).

For $C_{28}H_{23}N_5O_{12}NiEu$ (**II**)

Anal. calcd., %	C, 40.37	H, 2.76	N, 8.41
Found, %	C, 40.30	H, 2.72	N, 8.38

IR (ν, cm^{-1}): 1643 ν(COO^-), 1607 ν(C=O), 1557 ν(C=N).

X-ray crystallography. Single crystal X-ray diffraction analyses of **I** and **II** were carried out on a Bruker Smart Apex II CCD diffractometer equipped with a graphite monochromated MoK_α radiation (λ = 0.71073 Å) by using ϕ/ω scan technique at room temperature. Semi-empirical absorption corrections were applied using SADABS. All structure were solved by direct methods using the SHELXS program of the SHELXTL package and refined with SHELXL. Hydrogen atoms were added geometrically and refined with riding model position parameters and fixed isotropic thermal parameters. The crystallographic data and selected bond lengths and angles for **I** and **II** are listed in Tables 1 and 2, respectively.

Supplementary material for structures has been deposited with the Cambridge Crystallographic Data Centre (CCDC nos. 1587618 (**I**) and 1587619 (**II**); deposit@ccdc.cam.ac.uk or http://www.ccdc.cam ac.uk).

RESULTS AND DISCUSSION

Single-crystal X-ray diffraction analyses revealed that complexes **I** and **II** are isostructural and the fundamental building unit of the crystal structures is composed of $[Ln(NiL)(Nip)(C_2O_4)_{0.5} \cdot H_2O]$ (Ln = Er (**I**), Eu (**II**)) (Fig. 1a). The center Ln^{3+} ion is nine-coordinated and surrounded by two oxygen atoms from two macrocyclic oxamide groups, four oxygen atoms from three Nip^{2-}, two oxygen atoms from $C_2O_4^{2-}$ and the last one oxygen atom from coordination water molecule, the coordination geometry of Ln^{3+} ion is a distorted one capped square antiprism. The Ln–O distances are from 2.369(4) to 2.631(4) Å for **I**, 2.361(4) to 2.586(5) Å for **II**, while the OLnO bond angles are in the range of 50.98(13)°–151.35(13)° for **I**, 45.99(15)°–166.51(15)° for **II**. For all nickel ions, the coordination geometry is a distorted square planar, which surrounded by four nitrogen atoms from the macrocyclic oxamide group. The Ni–O distances and ONiO bond angles are in the range of 1.871(5)–1.912(4) Å and 87.05(19)°–165.7(2)° for **I**, 1.857(5)–1.905(5) Å and 86.8(2)°–165.9(2)° for **II**, respectively. The Ni^{2+} and Ln^{3+} ions are bridged by the macrocyclic oxamide ligand to form binuclear NiLn unit with Ni···Ln average separations 5.8430 for **I** and 5.8066 Å for **II**. Two adjacent NiLn units are connected by $C_2O_4^{2-}$ to form tetranuclear $[Ni_2Ln_2]$ unit, as shown in Fig. 1b, and Er···Er and Eu···Eu distances are 6.2616(13) and 6.2279(30) Å, respectively. Furthermore, adjacent tetranuclear $[Ni_2Ln_2]$ units are interlinked by two COO^- from two Nip^{2-} to form a one dimensional structure (Fig. 2a), and the adjacent chains are connected by Nip^{2-} to form a 2D layer architecture, as shown in Fig. 2b. In two-dimensional structure, each NiL acts as a terminal ligand to connect a Ln^{3+} ion via exo oxygen donors, each $C_2O_4^{2-}$ bridges two Ln^{3+} ions via four oxygen atoms, while each Nip^{2-} connects three Ln^{3+} ions with carboxylate groups, adopting μ_3-κ^2O,O′:κO″:κO‴ bridging coordination modes (see Scheme 1b). The adjacent 2D net-

Table 1. Crystallographic data and structure refinement for complexes **I** and **II**

Parameter	Value	
	I	**II**
Fw	847.48	832.18
Crystal system	Monoclinic	Monoclinic
Space group	*C*2/*c*	*C*2/*c*
a, Å	31.701(6)	31.43(2)
b, Å	11.189(2)	11.116(7)
c, Å	18.829(4)	18.728(11)
β, deg	126.076(3)	126.04(4)
V, Å^3	5398.1(18)	5291(6)
Z	8	8
ρ_{caled}, g/cm^3	2.086	2.089
Crystal size, mm	0.22 × 0.21 × 0.18	0.22 × 0.20 × 0.17
Goodness-F^2	1.091	1.008
Reflections collected/unique	17296/5581	16893/5473
R_{int}	0.0486	0.0833
R_1, wR_2 ($I > 2\sigma(I)$)*	0.0383, 0.0514	0.0463, 0.0844
R_1, wR_2 (all data)	0.0512, 0.0932	0.0753, 0.0890
Largest diff. peak and hole, *e* Å^{-3}	1.186 and −0.998	0.977 and −1.615

* $R_1 = \Sigma||F_o| - |F_c||/\Sigma|F_o|$, $wR_2 = \{\Sigma[w(F_o^2 - F_c^2)^2]/\Sigma[w(F_o)^2]\}^{1/2}$.

work architectures are linked together with C–H···O and/or O–H···O intermolecular hydrogen bonding to form a 3D supramolecular framework (Fig. 3). The data of hydrogen bonds for both complexes are listed in Table 3.

In this paper, use 5-nitroisophthalate and NiL as co-ligands to react with $Ln(NO_3)_3 \cdot 6H_2O$ (Ln = Er, Eu), two novel 3*d*–4*f* CPs **I**, **II** were obtained in the same reaction conditions. During the course of the reactions, some mononuclear macrocyclic oxamide complex NiL have been hydrolyzed to afford oxalate in basic conditions according to the previous reports [27]. Then $C_2O_4^{2-}$ acts as bridge ligand to react with $Ln(NO_3)_3 \cdot 6H_2O$ also, thus compounds **I** and **II** were prepared. Both complexes are stable and insoluble in water, alcohol, acetonitrile and *N*,*N*-dimethylformamide. The elemental analyses of **I** and **II** are also consistent with the results of single-crystal X-ray diffraction analyses. The IR spectra show strong peaks in the region 1635–1643 and 1607–1611 cm^{-1}, which are assigned to the ν(C=O) vibrations of carboxyl and oxamide groups, respectively [28]. The IR spectra exhibit strong absorption bands in the region 1541–1557 cm^{-1} due to the ν(C=N) vibrations [28]. The bands around 3421 cm^{-1} are characteristic of the hydroxyl from H_2O.

In order to study the effects of 5-nitroisophthalate, $C_2O_4^{2-}$ and NiL on the fluorescence of rare earth ions, the solid-state fluorescence spectra of complexes **I**, **II** and $Ln(NO_3)_3 \cdot 6H_2O$ (Ln = Er, Eu) were measured using the excitation wavelength of 280 nm for **I** and 300 nm for **II** under room temperature. The fluorescence spectra of complex **I** and $Er(NO_3)_3 \cdot 6H_2O$ were given in Fig. 4a. The main emission bands for the $Er(NO_3)_3 \cdot 6H_2O$ are at 542, 550, and 664 nm, and

Table 2. Selected bond distances (Å) and angles (deg) for complexes **I** and **II**

Bond	*d*, Å	Bond	*d*, Å
		I	
Er(1)–O(6)$^{\#1}$	2.369(4)	Er(1)–O(5)$^{\#2}$	2.411(4)
Er(1)–O(9)	2.455(4)	Er(1)–O(10)$^{\#3}$	2.491(4)
Er(1)–O(11)	2.466(4)	Er(1)–O(1)	2.554(4)
Ni(1)–N(3)	1.871(5)	Ni(1)–N(4)	1.912(4)
		II	
Eu(1)–O(5)	2.464(4)	Eu(1)–O(7)$^{\#1}$	2.361(4)
Eu(1)–O(9)$^{\#2}$	2.438(4)	Eu(1)–O(6)	2.398(4)
Eu(1)–O(3)	2.442(4)	Eu(1)–O(2)	2.539(5)
Ni(1)–N(3)	1.857(5)	Ni(1)–N(2)	1.905(5)
Angle	ω, deg	Angle	ω, deg
		I	
O(6)$^{\#1}$Er(1)O(5)$^{\#2}$	76.69(12)	O(5)$^{\#2}$Er(1)O(3)	99.56(13)
O(3)Er(1)O(11)	118.97(13)	O(5)$^{\#2}$Er(1)O(2)	129.09(13)
O(3)Er(1)O(4)	50.98(13)	O(10)$^{\#3}$Er(1)O(4)	108.81(13)
O(9)Er(1)O(11)	144.81(13)	O(1)Er(1)O(4)	69.54(12)
N(1)Ni(1)N(4)	87.05(19)	N(3)Ni(1)N(1)	165.7(2)
		II	
O(7)$^{\#1}$Eu(1)O(6)	76.25(14)	O(7)$^{\#1}$Eu(1)O(9)$^{\#2}$	151.04(14)
O(6)Eu(1)O(3)	139.37(14)	O(7)$^{\#1}$Eu(1)O(1)	67.98(15)
O(3)Eu(1)O(5)	144.42(15)	O(9)$^{\#2}$Eu(1)O(8)$^{\#2}$	51.57(14)
O(6)Eu(1)O(1)	128.85(14)	O(4)$^{\#3}$Eu(1)O(8)$^{\#2}$	108.63(14)
N(1)Ni(1)N(2)	86.8(2)	N(4)Ni(1)N(2)	164.2(2)

* Symmetry transformations used to generate equivalent atoms: $^{\#1}$ $x, y + 1, z$; $^{\#2}$ $-x + 1, -y + 1, -z + 1$; $^{\#3}$ $-x + 1, y, -z + 1/2$ (**I**); $^{\#1}$ $-x, -y + 2, -z$; $^{\#2}$ $-x, -y + 1, -z$; $^{\#3}$ $-x, y, -z + 1/2$ (**II**).

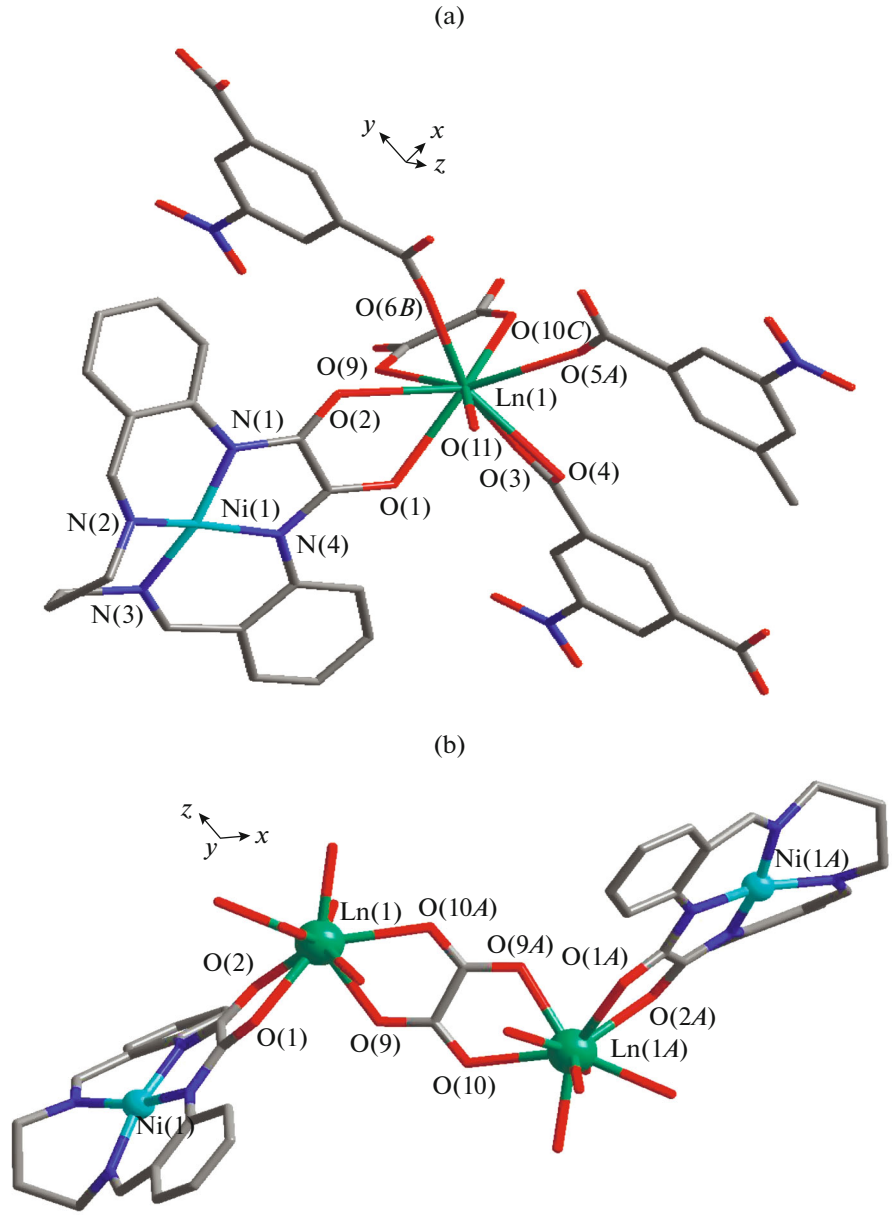

Fig. 1. Portion of the crystal structure of **I** and **II** showing the coordinate environments of Ln(III) (Ln = Er (**I**), Eu (**II**)) and Ni^{2+} ions; all H atoms are omitted for clarity; symmetry codes: (*A*) $1-x, y, 0.5-z$; (*B*) $x, 1+y, z$; (*C*) $1-x, 1-y, 1-z$ (a); perspective view of Ni_2Ln_2 unit, hydrogen atoms, Nip^{2-} ligands were removed for clarity (b).

these bands may be attributed to the $^2H_{11/2} \rightarrow {}^4I_{15/2}$, $^4S_{3/2} \rightarrow {}^4I_{15/2}$, and $^4F_{9/2} \rightarrow {}^4I_{15/2}$ transitions of the Ln^{3+} ion, respectively. Compared with the emission spectra of the $Er(NO_3)_3 \cdot 6H_2O$, these fluorescence intensity of complex **I** at 542, 550, and 664 nm decrease or disappear. The fluorescence spectra of the complex **II** and $Eu(NO_3)_3 \cdot 6H_2O$ were given in Fig. 4b. $Eu(NO_3)_3 \cdot 6H_2O$ exhibits fluorescence bands at 594, 618, 669 and 689 nm, which are attributable to $^5D_0 \rightarrow {}^7F_1$, $^5D_0 \rightarrow {}^7F_2$, $^5D_0 \rightarrow {}^7F_3$ and $^5D_0 \rightarrow {}^7F_4$ transitions of the Ln^{3+} ion, respectively. Compared with the emission spectra of the $Eu(NO_3)_3 \cdot 6H_2O$, these fluorescence intensity of **II** decrease or disappear. For complexes **I** and **II**, the fluorescence measurement proved that the phenomenon of fluorescence quenching happened, which maybe attribute to the energy transfer from the

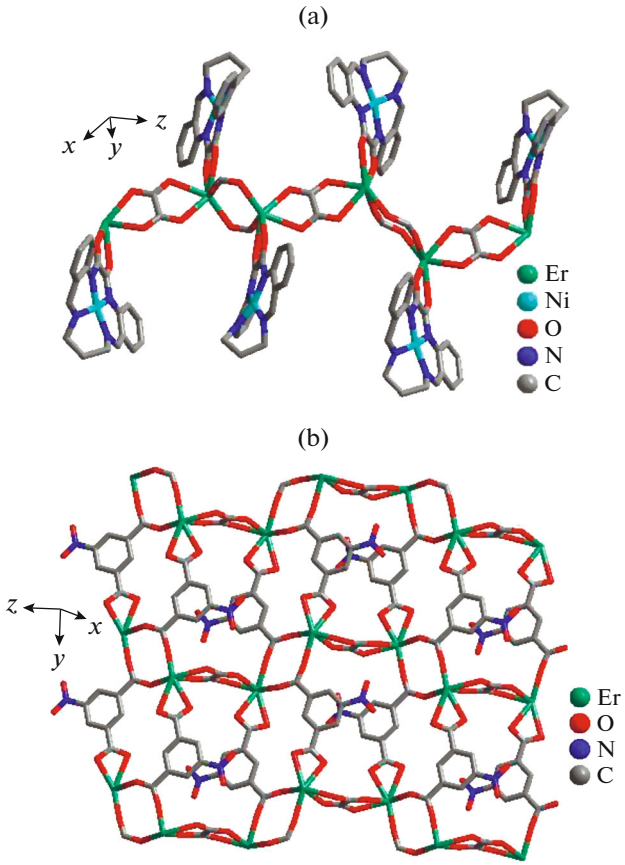

Fig. 2. View of the self-assembly a chain constructed by $[Er(NiL)(Nip)(C_2O_4)_{0.5} \cdot H_2O]$, water, hydrogen atoms and Nip^{2-} ligands were removed for clarity (a); view of the self-assembly 2D sheet structure, hydrogen atoms, water and NiL ligands were removed for clarity (b).

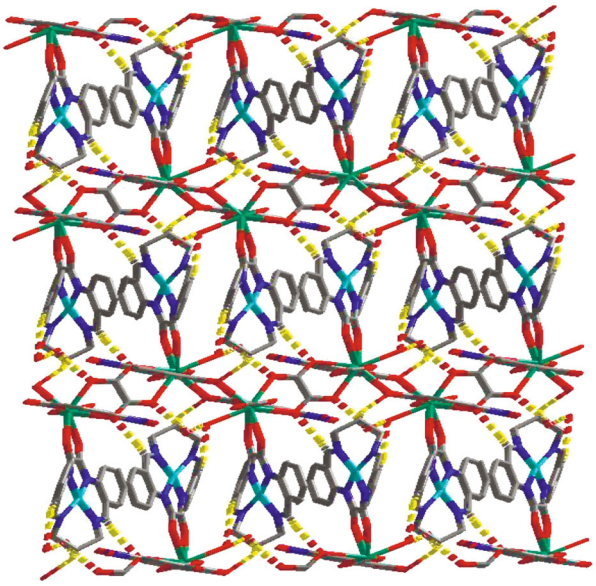

Fig. 3. View of the supermolecule framework through hydrogen bond interactions in **I** and **II**.

excited Er(III) or Eu(III) to the Ni(II) center through the oxamidic oxygen bridges [23, 25].

In summary, two novel 3*d*–4*f* CPs $[Ln(NiL)(Nipt)(C_2O_4)_{0.5} \cdot H_2O] \cdot H_2O$ (Ln = Er (**I**), Eu (**II**) were obtained by using 'metalloligand' and co-ligand synthetic approach under solvothermal conditions. The structure shows that bridge ligands Nip^{2-} and

Table 3. Geometric parameters of hydrogen bonds for **I** and **II***

D–H···A	Distance, Å			Angle DHA, deg
	D–H	H···A	D···A	
		I		
O(11)–H(11*A*)···O(12)$^{\#1}$	0.85	1.79	2.631(6)	1689
O(11)–H(11*B*)···O(7)$^{\#2}$	0.85	2.43	3.228(6)	157
O(12)–H(12*A*)···O(10)$^{\#3}$	0.86	2.05	2.902(6)	170
C(9)–H(9*A*)···O(5)$^{\#1}$	0.97	2.46	3.358(7)	153
C(11)–H(11)···O(9)$^{\#2}$	0.93	2.35	3.276(7)	172
		II		
O(5)–H(5*A*)···O(10)$^{\#1}$	0.96	2.44	3.207(7)	137
O(5)–H(5*B*)···O(12*w*)	0.84	1.79	2.608(7)	166
O(12*w*)–H(12*A*)···O(4)$^{\#2}$	0.85	2.04	2.876(7)	167
C(9)–H(9)···O(3)$^{\#3}$	0.93	2.33	3.254(8)	170
C(11)–H(11*A*)···O(6)$^{\#4}$	0.97	2.44	3.338(8)	153
C(11)–H(11*B*)···O(10)$^{\#5}$	0.97	2.56	3.274(9)	131

*Symmetry transformations used to generate equivalent atoms: $^{\#1}$ $1/2 - x, 1/2 + y, 1/2 - z$; $^{\#2}$ $x, 1 - y, 1/2 + z$; $^{\#3}$ $1/2 - x, 3/2 - y, -z$ (**I**); $^{\#1}$ $-x, y, -1/2 - z$; $^{\#2}$ $x, 2 - y, -1/2 + z$; $^{\#3}$ $1/2 - x, 3/2 - y, 1 - z$; $^{\#4}$ $1/2 + x, 3/2 - y, 1/2 + z$; $^{\#5}$ $1/2 + x, 1/2 + y, 1 + z$ (**II**).

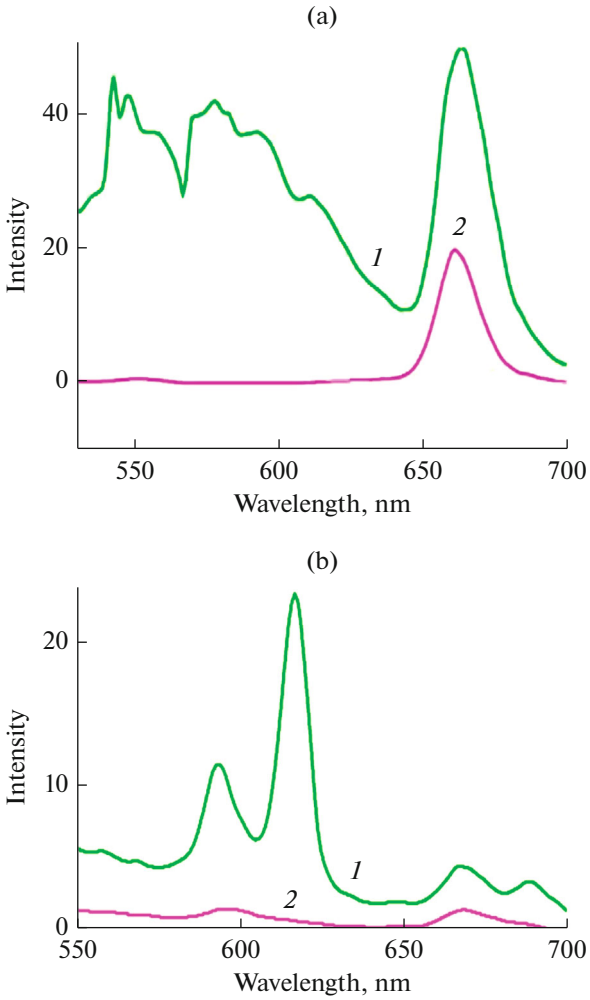

Fig. 4. The fluorescence spectra: (a) $Er(NO_3)_3 \cdot 6H_2O$ (*1*), **I** (*2*); (b) $Eu(NO_3)_3 \cdot 6H_2O$ (*1*), **II** (*2*).

$C_2O_4^{2-}$ play an important role in the formation of 2D network architecture, and adjacent 2D framework are linked together with C–H···O and/or O–H···O intermolecular hydrogen bonding to form a 3D supramolecular framework. The fluorescence properties of the complexes **I** and **II** were also studied.

ACKNOWLEDGMENTS

This work was supported by the National Natural Science Foundation of China (no. 20771083) and Tianjin Normal University (no. 52XC1102).

REFERENCES

1. Sharples, J.W. and Collison, D., *Coord. Chem. Rev.*, 2014, vol. 260, p. 1.
2. Sun, Y.G., Zong, W.H., Xiong, G., et al., *Polyhedron*, 2014, vol. 83, p. 68.
3. Zhang, X.L., Chen, C., Liu, X.L., et al., *J. Solid State Chem.*, 2017, vol. 253, p. 360.
4. Tan, X., Ji, X., and Zheng, J.M., *Inorg. Chem. Commun.*, 2015, vol. 60, p. 27.
5. Xie, W.P., Wang, N., Long, Y., et al., *Inorg. Chem. Commun.*, 2014, vol. 40, p. 151.
6. Tao, C.H., Ma, J.C., Zhu, L.C., et al., *Polyhedron*, 2017, vol. 128, p. 38.
7. Feng, X., Ling, X.L., Liu, B., et al., *Inorg. Chem. Commun.*, 2012, vol. 20, p. 1.
8. Liu, X., Jiang, J.Z., Jia, Y.S., et al., *Appl. Surf. Sci.*, 2017, vol. 412, p. 279.
9. Jiang, Y.Q., Fan, X.L., Xiao, X.Z., et al., *Int. J. Hydrogen. Energ.*, 2017, vol. 42, p. 9353.
10. Hu, H.C., Kang, X.M., Cao, C.S., et al., *Chem. Commun.*, 2015, vol. 51, p. 10850.
11. Wu, Z.L., Dong, J., Ni, W., et al., *Inorg. Chem.*, 2015, vol. 54, p. 5266.
12. Yang, T.H., Silva, A.R., Fu, L.S., and Shi, F.N., *Dalton Trans.*, 2015, vol. 44, p. 13745.
13. Zhao, B., Cheng, P., Chen, X.Y., et al., *J. Am. Chem. Soc.*, 2004, vol. 126, p. 3012.
14. Feng, R., Chen, L., Chen, Q.H., et al., *Cryst. Growth Des.*, 2011, vol. 11, p. 1705.
15. Gao, H.L., Yi, L., Ding, B., et al., *Inorg. Chem.*, 2006, vol. 45, p. 481.
16. He, X.X., Liu, Y., Lv, Y., et al., *Inorg. Chem.*, 2016, vol. 55, p. 2048.
17. Xin, N., Sun, Y.Q., Zheng, Y.F., et al., *J. Solid State Chem.*, 2016, vol. 243, p. 267.
18. Black, D.S.C., Vanderzalm, C.H.B., and Hartshorn, A.J., *Inorg. Nucl. Chem. Lett.*, 1976, vol. 12, p. 657.
19. Zhang, D.J., Yu, Y.Z., Wang, J.J., et al., *Polyhedron*, 2016, vol. 117, p. 703.
20. Zheng, S.R., Tan, J.B., Cai, S.L., et al., *CrystEngComm*, 2016, vol. 18, p. 8672.
21. Liu, J., Zhang, H.B., Tan, Y.X., et al., *Inorg. Chem.*, 2014, vol. 53, p. 1500.
22. Li, H.R., Sheng, T.I., Xue, Z.Z., et al., *CrystEngComm*, 2017, vol. 19, p. 2106.
23. Berner, V.G., Darnall, D.W., and Birnbaum, E.R., *Biochem. Biophys. Res. Commun.*, 1975, vol. 66, p. 763.
24. Higashiyama, N. and Adachi, G., *Chem. Lett.*, 1990, vol. 19, p. 2029.
25. Saksmoto, M., Hashimura, M., Nakayama, Y., et al., *Bull. Chem. Soc. Jpn.*, 1992, vol. 65, p. 1162.
26. Winpenny, R.E.P., *Chem. Soc. Rev.*, 1998, vol. 27, p. 447.
27. Ruiz, R., Faus, J., Lloret, F., et al., *Coord. Chem. Rev.*, 1999, vol. 195, p. 1069.
28. Nakamoto, K., *Infrared, Raman Spectra of Inorganic and Coordination Compounds*, Pt. B., New York: Wiley, 1997.